

High-doping performance of sulfur and zinc dopants for tunnel diodes using hydride vapor phase epitaxy

Ryuji Oshima¹, Yasushi Shoji¹, Kikuo Makita¹, Akinori Ubukata², Takeyoshi Sugaya¹

¹ National Institute of Advanced Industrial Science and Technology, Tsukuba, Ibaraki, 305-8568, Japan

² Taiyo Nippon Sanso Corporation, Tsukuba, Ibaraki, 305-2611, Japan

Abstract — We evaluate the high-doping performances of sulfur (S) and zinc (Zn) as *n*- and *p*-type dopants by hydride vapor phase epitaxy (HVPE) to develop tunnel diodes (TDs), which is used for the interconnection in multi-junction solar cells. HVPE has emerged as a low-cost alternative for the fabrication of III-V solar cells. For *p*-GaAs, all the Zn atoms can be activated and free-hole concentrations with $>10^{19} \text{ cm}^{-3}$ could be realized. Contrary, the free-electron concentration was saturated at $5 \times 10^{18} \text{ cm}^{-3}$ for *n*-GaAs due to the formation of $V_{\text{Ga}}\text{-S}_{\text{As}}$ complexes. Nevertheless, GaAs TDs with excessive S incorporation with a density of $4 \times 10^{19} \text{ cm}^{-3}$ yields a peak tunneling-current density of 5 A/cm^2 . Previously, we developed a triple-chamber HVPE and achieved conversion efficiencies of 20.8% for GaAs and 12.1% for InGaP cells. By integrating these components together in a single growth, we develop a InGaP/GaAs dual-junction solar cell showing the conversion efficiency of 21.8% with a minimal voltage loss in TDs under at least 1sun operation.

Index Terms — Photovoltaic cells, III-V semiconductor materials, hydride vapor-phase epitaxy (HVPE), multi-junction solar cells

I. INTRODUCTION

THE conversion efficiency (η) of III-V solar cells steadily increases through the use of multijunction structures [1]. Monolithic InGaP/GaAs dual-junction solar cells (DJSCs) have been studied extensively owing to their excellent bandgap combination in lattice-match systems, exhibiting $\eta = 31.6\%$ under 1-sun illumination [2]. Moreover, inverted metamorphic InGaAsP/InGaAs solar cells in lattice-mismatch system recently achieved the highest η of 32.6% under 1-sun illumination [3]. According to these techniques, various studies based on three or more junctions have been conducted with an objective of increasing η [4]-[8].

Despite a superior device performance compared to prevalent materials such as Si, these high-efficiency devices are currently limited to high-value applications, such as space [9] and high-concentration systems [10], owing to their high manufacturing cost that arises from the utilization of incumbent metal-organic vapor phase epitaxy (MOVPE). The manufacturing cost associated with the material growth should be lowered to enable their large-scale terrestrial applications, such as rooftops, vehicles, unmanned aerial vehicles, and

portable power, while simultaneously maintaining the high conversion efficiency [11].

Recently, the hydride vapor phase epitaxy (HVPE) has been given much attention as an alternative to MOVPE because of a potential to lower the growth costs. In HVPE, cost-effective metal-chlorides are utilized to derive group-III atoms instead of metalorganics. Furthermore, the growth under a lower V/III ratio of ~ 2 is possible [12], resulting in significant saving in input costs. In addition, it can provide higher throughput with a growth rate of several hundred $\mu\text{m/h}$ [13],[14]. However, HVPE in a single growth chamber traditionally had difficulty in producing complex devices with abrupt heterointerfaces, because in-situ generation of group III metal-chlorides cannot be change abruptly as in MOVPE [15]. To overcome this issue multi-chamber reactors have been developed. Simon et al. developed a double-chamber, vertical HVPE system and fabricated efficient GaAs cells that possess abrupt heterointerfaces [16].

Previously, we developed a laminar flow-type, triple-chambered vertically positioned vertically vertical flow-type [17].

In two-terminal InGaP/GaAs DJSCs, η of 20.8% [18] and InGaP/GaAs DJSCs with η of 23.7% [23,24]. In HVPE-grown InGaP using dimethylzinc (DMZn) and *n*-type dopants, high-doping performance was demonstrated using *p*-type dopants [2]. InGaP/GaAs DJSCs with η of 23.7% [23,24]. In HVPE-grown InGaP using dimethylzinc (DMZn) and *n*-type dopants, high-doping performance was characterized the

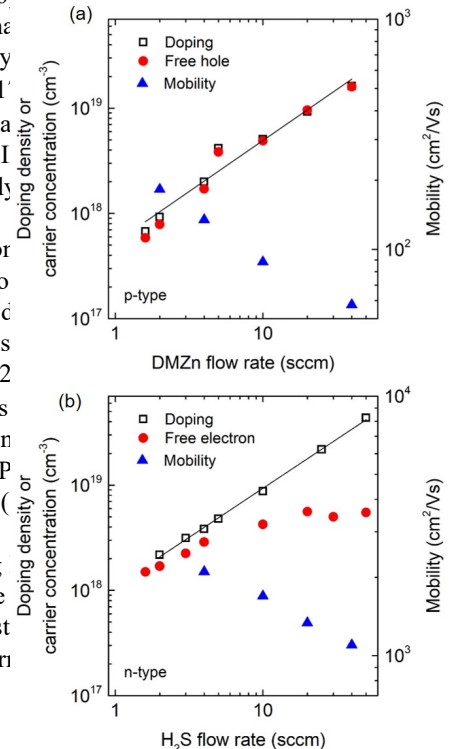


Fig. 2 Doping densities, free-carrier concentrations, and mobilities of *p*- and *n*-type GaAs films as a function of dopant-gas flow.

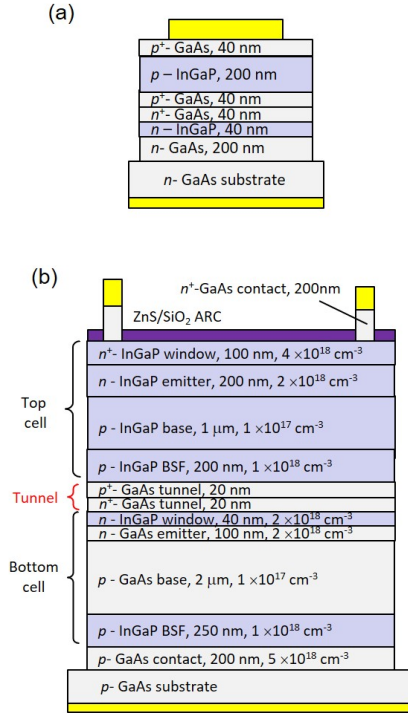


Fig. 1 Structural schematics of (a) GaAs TDs and (b) InGaP/GaAs DJSCs.

InGaP/GaAs DJSCs by integrating these components together in a single growth.

II. EXPERIMENTAL PROCEDURE

III–V materials and devices were grown on 2-inch diameter GaAs (001) substrates miscut 4° toward the (111)B direction in a custom-built hot-wall reactor (Taiyo Nippon Sanso, H260) at atmospheric pressure [17–19]. The source and substrate regions were heated to 850°C and 660°C , respectively. Gaseous hydrogen chloride (HCl), gallium (Ga) and indium (In) metals, arsine (AsH_3), and phosphine (PH_3) were utilized to grow III–V layers. Dimethylzinc (DMZn) (200 ppm) and hydrogen sulfide (H_2S) (200 ppm) in a hydrogen (H_2) mixture were utilized as the p - and n -type dopants, respectively. The growth rates of GaAs and InGaP were 12 and 24 $\mu\text{m}/\text{h}$, respectively, and the total flow rate of the H_2 -carrier gas was 6 SLM.

A series of p - and n -type GaAs films were grown with different DMZn and H_2S dopant flows to evaluate the doping performance under the standard growth conditions [18]. The thickness was approximately 1 μm . Carrier concentrations, doping densities, and mobilities were determined using electrochemical capacitance-voltage, secondary-ion mass spectrometry, and van der Pauw Hall effect measurements, respectively. Then, GaAs TD structures, GaAs single junction solar cells and InGaP/GaAs DJSCs were fabricated. The TD structure, as shown in Fig. 1(a), mimics the InGaP/GaAs DJSC structure shown in Fig. 1(b), except the thickness of each p^+ -

and n^+ -GaAs tunnel layers. The detailed growth condition of both GaAs and InGaP subcells was described in refs. [18] and [19]. We note that the InGaP top cell does not have a widegap window layer to passivate the surface recombination because aluminum source is not equipped in our HVPE system at this time.

After the HVPE growth of the device structures, AuGeNi/Au and Ti/Au electrodes were formed as n - and p -type ohmic contacts using electron-beam evaporation. The metallization was performed at 350°C for 2 mins with ambient nitrogen. Mesa isolation was performed using a standard photolithography system. ZnS/ SiO_2 bi-layer antireflection coating (ARC) was deposited onto the cell via radio-frequency magnetron sputtering. The cell size and TD pads were 0.1 and 0.002 cm^2 , respectively. The external quantum efficiency (EQE) was measured with a chopped, monochromatic light with a constant photon flux of $1 \times 10^{14} \text{ cm}^{-2}$. The current–voltage (I – V) characteristics were measured in a dark environment under an air mass of 1.5 global (AM1.5G) with illumination of 1 sun.

III. RESULTS AND DISCUSSION

A. High Doping Performance

Figure 2 shows the doping density, free-carrier concentration, and mobility as functions of dopant-gas flow for both dopants. For p -GaAs, first-order

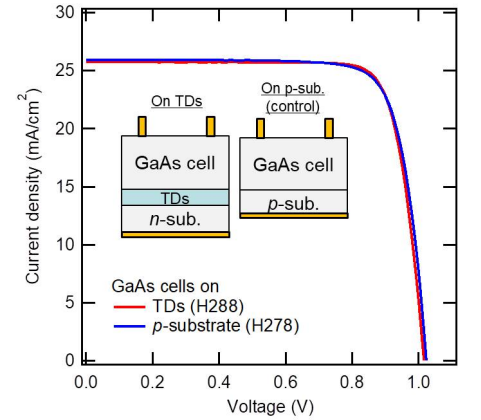


Fig. 4 I – V characteristics measured under light (1 sun) for GaAs solar cells grown on GaAs TDs and p -substrates.

dependence is obtained. The free-hole concentration was in agreement with the incorporation of Zn atoms, indicating that all the Zn atoms in the GaAs layers could be activated and free-hole concentrations with $>10^{19} \text{ cm}^{-3}$ could be realized, which was high enough to degenerate doping. On the contrary, for n -GaAs, approximately 70% of S atoms could be electrically activated for a H_2S flow of 2 sccm and the activation rate was monotonically decreased with increasing the H_2S flow. The free-electron concentration was consequently saturated at $\sim 5 \times 10^{18} \text{ cm}^{-3}$ for a H_2S flow of larger than 10 sccm, though the electron mobility was

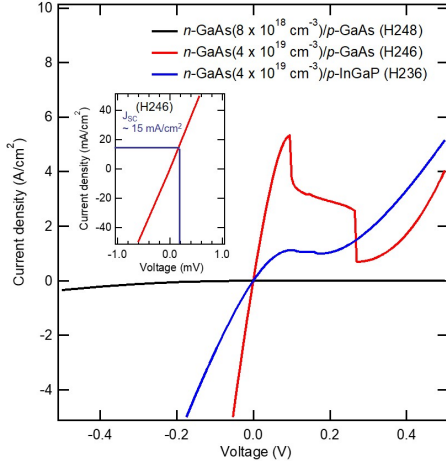


Fig. 3 I - V curves for p^+ -GaAs/ n^+ -GaAs and p^+ -InGaP/ n^+ -GaAs TDs grown with different S-doping densities in n^+ -GaAs layers. The inset shows the enlarged I - V curve measured around 0 V for H246.

decreased with increasing the doping density. In a separate measurement of atomic force microscope (not shown), all the films with various doping density showed similar root mean square roughness of less than 1 nm without any precipitates. In a previously reported study, it was argued that S-doped GaAs grown using VPE was compensated by the S_{As} - V_{Ga} acceptor complexes at all the doping levels, where S_{As} and V_{Ga} denote S atoms at As sites and vacancies at Ga sites, respectively [26],[27]. Additionally, the compensation ratio, i.e. the relative density of acceptor complexes, increased with an increase in the H_2S flow, resulting in the saturation of free-electron concentration. These were similar to our own observations. Thus, a high free-electron concentration in excess of 10^{19} cm^{-3} was found to be difficult in our standard growth condition using S dopants, and other dopant elements, such as Se [22] or tellurium [28],[29], should be examined.

B. Characterization of GaAs TDs

We evaluated HVPE-grown n^+/p^+ -GaAs TDs using S and Zn dopants. The free-hole concentration in the p^+ -GaAs layers was fixed to $2 \times 10^{19} \text{ cm}^{-3}$. Although the free-electron concentration was saturated at $5 \times 10^{18} \text{ cm}^{-3}$, we fabricated TDs with 2 kinds of S-doped GaAs layers with a density of $8 \times 10^{18} \text{ cm}^{-3}$ or $4 \times 10^{19} \text{ cm}^{-3}$. As shown in Fig. 3, I - V curves exhibited quite different results and the TD with an S-doping density of $4 \times 10^{19} \text{ cm}^{-3}$ showed a typical Esaki-type tunnel behavior [20],[21] with a peak tunneling-current density of 5 A/cm^2 . This suggests that some fraction of S atoms could be activated in highly biased TDs and/or a certain number of V_{Ga} - S_{As} complexes could transfer current via the deep level at the junction [30]. In any case, when the InGaP/GaAs DJSCs operate under a typical short-circuit current density (J_{SC}) of $\sim 15 \text{ mA/cm}^2$, the series resistance in the TD is estimated to be $13 \mu\Omega/\text{cm}^2$ leading to the open-circuit voltage (V_{OC}) drop of less than $200 \mu\text{V}$ [2] at an illumination of 1 sun as shown in the inset

of Fig. 3. For InGaP/GaAs DJSC, however, GaAs TDs parasitically absorb the light, leading to the reduction of the J_{SC} of the GaAs subcell located underneath the TD. Thus, the development of TDs with wider bandgap materials will be necessary to improve the transparency. Fig. 3 also shows the I - V curve measured for n^+ -GaAs/ p^+ -InGaP TDs. The doping density of p^+ -InGaP layer was approximately $2 \times 10^{19} \text{ cm}^{-3}$. This TD yielded a peak tunneling-current density of 1.1 A/cm^2 , which was lower by a factor of five than that for the GaAs TD. In a characterization of the Zn-doped InGaP film, the free-hole concentration was determined to be $5 \times 10^{18} \text{ cm}^{-3}$, which was much lower than the doping density. Thus, a small tunneling current in GaAs/InGaP TDs was likely to be due to poor activation ratio of Zn atoms in InGaP films. Improving the doping performance in InGaP films is ongoing and hereafter, we used GaAs TDs for the cell fabrication.

C. GaAs solar cells grown on tunnel junction

Then, we characterize the effect of GaAs TDs on the cell performance using GaAs single junction solar cells. As shown in the inset of Fig. 4,

we fabricated a pair of GaAs solar cells that were nominally identical, except that one structure incorporated a TD between the rear of the active region and the n -GaAs substrate, and the other was the control cell grown on the p -GaAs substrate as described in ref. [18]. From the I - V measurement under 1sun illumination, the cell grown on TDs showed $\eta = 21.2\%$ with $J_{SC} = 25.7 \text{ mA/cm}^2$, $V_{OC} = 1.02 \text{ V}$, and fill factor (FF) = 0.81, which was quite similar with the control cell showing $\eta = 20.9\%$ with $J_{SC} = 25.6 \text{ mA/cm}^2$, $V_{OC} = 1.02 \text{ V}$, and (FF) = 0.80. In addition, there was no change in EQE spectra (not shown) within the error of the measurements. Thus, we never see any reason to

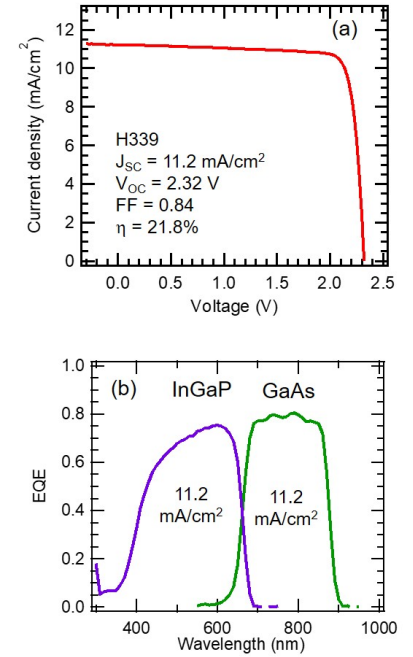


Fig. 5(a) I - V curves and (b) EQE measurements for InGaP/ GaAs DJSCs.

degrade the cell performance by the introduction of TDs. TDs fabricated in our HVPE effectively acts as a low-resistance interconnection with negligible impact on V_{OC} under at least 1 sun operation.

D. InGaP/GaAs DJSC Performance

Finally, InGaP/GaAs DJSCs was fabricated using GaAs TDs. As shown in fig. 1(b), we note that thinner thickness of 20 nm was used for each n^+ and p^+ -tunnel layer to reduce the parasitic absorption in the TDs. Figure 5(a) shows $I-V$ curves under an AM1.5G at 1 sun for DJSCs. The DJSC yielded an η value of 21.8% at 1 sun with $J_{SC} = 11.2$ mA/cm², $V_{OC} = 2.32$ V, and FF = 0.84. The obtained V_{OC} was within the expected range of values when taking the individual V_{OC} of 1.0 V for the GaAs [18] and 1.32 V for the InGaP cells [19] into account. Fig. 5(b) shows EQE of the InGaP top and GaAs bottom cells. A projected J_{SC} calculated by the integration of EQE of the top cell with the solar spectrum was 11.2 mA/cm², which was well matched to that of the GaAs bottom cell. However, the relatively small value of J_{SC} compared to the state-of-the-art DJSCs [2] was attributed to an unoptimized cell structure. For the InGaP top cell, the small EQE in shorter wavelength region was due to the lack of a surface passivation leading to a high surface recombination velocity [19]. To improve the device performance of the top cell, either an introduction of wide bandgap window layer or thinner emitter layer [23] would be effective. For this, future work will focus on the development of the Al-contained material in HVPE [31]. For the GaAs bottom cells, improving the transparency in the TDs by the use of wider bandgap materials would lead to an increase in the EQE of the bottom cell.

IV. CONCLUSION

Herein, we characterized the high-doping performance of GaAs films doped with Zn and S atoms. All the Zn atoms in GaAs layers could be activated while the free-electron concentration was saturated at $\sim 5 \times 10^{18}$ cm⁻³ due to the $S_{As}-V_{Ga}$ acceptor complexes. However, GaAs TDs with excessive incorporation of S with a density of 4×10^{19} cm⁻³ provided a peak current of 5 A/cm². Consequently, we successfully fabricated the InGaP/GaAs DJSC with a minimal voltage loss in TDs under at least 1 sun operation. Though there is a large window to improve the cell performance in our HVPE-grown DJSC, this study is a major step toward the development of the highly efficient III-V multi-junction solar cells grown using a cost-effective HVPE technique.

ACKNOWLEDGMENT

This study was supported by the New Energy and Industrial Technology Development Organization (NEDO).

REFERENCES

- [1] M. A. Green, *et al.*, "Solar cell efficiency tables (version 53)" *Prog. Photovolt. Res. Appl.*, vol. 27, pp.3-12, 2019.
- [2] B. M. Kayes, L. Zhang, R. Twist, I. K. Ding, and G. S. Higashi, "Flexible thin-film tandem solar cells with >30% efficiency," *IEEE J. Photovolt.*, vol. 4, no. 2, pp. 729-733, Mar. 2014.
- [3] N. Jain *et al.* "High-efficiency inverted metamorphic 1.7/1.1 eV GaInAsP/GaInAs dualjunction solar cells" *Appl. Phys. Lett.*, vol 113, pp. 053905-1-053905-3.
- [4] K. Sasaki, *et al.*, "Development of InGaP/GaAs/InGaAs inverted triple junction concentrator solar cells" *AIP Conf. Proc.*, vol. 1556, pp. 22-25, 2013.
- [5] J. F. Geisz, *et al.*, "Building a six-junction inverted metamorphic concentrator solar cell" *IEEE J. Photovolt.*, vol. 8, no. 2, pp. 626-632, Mar. 2018.
- [6] F. Dimroth *et al.*, "Four-junction wafer-bonded concentrator solar cells" *IEEE J. Photovolt.*, vol. 6, no. 1, pp. 343-349, Jan. 2016.
- [7] P. T. Chiu *et al.*, "35.8% space and 38.8% terrestrial 5J direct bonded cells" *Proc. 40th IEEE Photovoltaic Specialist Conference*, Denver, June, pp. 11-13, 2014.
- [8] V. Sabnis, H. Yuen, and M. Wiemer, "High-efficiency multijunction solar cells employing dilute nitrides" *AIP Conf. Proc.*, vol. 1477, pp. 14-19, 2012.
- [9] R. R. King *et al.*, "Advanced III-V multijunction cells for space" *Proc. IEEE 4th World Conf. Photovolt. Energy Conf.*, Waikoloa, HI, USA, pp.1757-1762, 2006,
- [10] D. C. Law *et al.*, "Future technology pathways of terrestrial III-V multijunction solar cells for concentrator photovoltaic systems" *Sol. Energy Mater. Sol. Cells*, vol. 94, no. 8, pp. 1314-1318, Aug. 2010.
- [11] T. Masuda *et al.*, "Next environment-friendly cars: Application of solar power as automobile energy source" *Proc. 43rd IEEE Photovoltaic Spec. Conf.*, Portland, June, pp. 0580-0584, 2016.
- [12] M. Ettenberg, G. H. Olsen, and C. J. Nuese "Effect of gas phase stoichiometry on the minority carrier diffusion length in vapor grown GaAs". *Appl. Phys. Lett.*, vol. 29, pp. 141-142, 1976.
- [13] K. Grüter, M. Deschler, H. Jürgensen, R. Beccard, and P. Balk, "Deposition of high quality GaAs films at fast rates in the LP-CVD system" *J Crystal Growth*, vol. 94, pp. 607-612, 1989.
- [14] L. Hollan and J. M. Durand, "Fast growth in GaAs VPE at low temperature and high partial pressures" *J Crystal Growth*, vol. 46, pp. 665-670, 1979.
- [15] S. N. G. Chu *et al.*, "Gallium contamination of InP epitaxial layers in InP/InGaAsP multilayer structures grown by hydride transport vapor phase epitaxy", *J. Electrochem. Soc.*, vol. 132, pp. 1187-1193, 1985.
- [16] J. Simon *et al.*, "Upright and Inverted Single-Junction GaAs Solar Cells Grown by Hydride Vapor Phase Epitaxy" *IEEE J. Photovolt.*, vol. 7, pp. 157-161, 2017.
- [17] R. Oshima, K. Makita, A. Ubukata, and T. Sugaya, "Fabrication of GaAs solar cells grown with InGaP layers by hydride vapor-phase epitaxy," *Jpn. J. Appl. Phys.*, vol. 57, p. 08RD06, 2018.
- [18] R. Oshima, K. Makita, A. Ubukata, and T. Sugaya, "Improvement of heterointerface properties of GaAs solar cells grown with InGaP Layers by hydride vapor-phase epitaxy," *IEEE Journal of Photovoltaics*, vol. 9, pp. 154-159, 2019.
- [19] Y. Shoji, R. Oshima, K. Makita, A. Ubukata, and T. Sugaya, "Ultrafast growth of InGaP solar cells via hydride vapor phase epitaxy" *Appl. Phys. Express*, vol. 12, p. 052004, 2019.
- [20] L. Esaki, "New phenomenon in narrow germanium on junctions," *Phys. Rev.*, vol. 109, pp. 603-604, 1958.
- [21] S. M. Bedair, M. F. Lamorte, and J. R. Hauser, "A two-junction cascade solar-cell structure" *Appl. Phys. Lett.*, vol. 34, pp. 38-39, 1979.
- [22] A. J. Ptak, J. Simon, K. L. Schulte, and N. Jain, "Tunnel junction development using hydride vapor phase epitaxy," *IEEE Journal of Photovoltaics*, vol. 8, pp. 322-326, 2018.
- [23] K. L. Schulte, J. Simon, and A. J. Ptak, "Multijunction Ga_{0.5}In_{0.5}P/GaAs solar cells grown by dynamic hydride vapor phase epitaxy," *Prog. Photovolt. Res. Appl.*, vol. 26, pp. 1-7, 2018.
- [24] J. Simon *et al.*, "III-V-based optoelectronics with low-cost dynamic hydride vapor phase epitaxy" *Crystals*, vol. 9(1), p. 3, 2019.
- [25] H. Sodabanlu, K. Watanabe1, M. Sugiyama, and Y. Nakano, "Effects of various dopants on properties of GaAs tunneling junctions and p-i-n solar cells," *Jpn. J. Appl. Phys.*, vol. 56, p. 08MC11, 2017.

- [26] R. Venkatasubramanian and S. K. Ghandhi, "Compensation mechanism in n⁺-GaAs doped with sulphur" *J. Crystal Growth*, vol. 97, pp. 827-832, 1989.
- [27] E. Veuhoff, M. Maier, K. H. Bachem, and P. Balk, "Sulfur incorporation in VPE GaAs" *J. Crystal Growth*, vol. 53, pp. 598-604, 1981.
- [28] G. Hamon, N. Paillet, J. Alvarez, A. Larrue, and J. Decobert, "Te doping of GaAs and GaInP using diisopropyl telluride (DIPTe) for tunnel junction applications" *J. Crystal Growth*, vol. 498, pp. 301-306, 2018.
- [29] S. Z. Sun, E. A. Armour, K. Zheng and C. F. Schaus, "Zinc and tellurium doping in GaAs and Al_xGa_{1-x}As grown by MOCVD" *J. Crystal Growth*, vol. 113, pp. 103-112, 1991.
- [30] K. Jandieri, et al., "Resonant electron tunneling through defects in GaAs tunnel diodes" *J. Appl. Phys.*, vol. 104, p. 094506, 2008.
- [31] A. Koukitu, F. Satoh, T. Yamane, H. Murakami, and Y. Kumagai, "HVPE growth of Al_xGa_{1-x}N ternary alloy using AlCl₃ and GaCl" *J. Crystal Growth*, vol. 305, pp. 335-339, 2007.